

Global motion coherence can influence the representation of ambiguous local motion

Peter Scarfe

Department of Cognitive, Perceptual and Brain Sciences,
University College London, UK



Alan Johnston

Department of Cognitive, Perceptual and Brain Sciences,
University College London, UK



Early cortical responses to visual motion are inherently ambiguous as to underlying motion in the world. This ambiguity derives from the fact that directionally selective cells in early visual areas, such as V1, can predominantly signal only 1D motion orthogonal to image contours spanning their small, spatially localized, receptive fields. One way in which local ambiguity could be overcome is by integrating motion signals over orientation and space. Here, we show that the direction of an aftereffect produced by ambiguous local motion signals is modified to be more consistent with the global motion of which the local signals were part. This suggests an architecture whereby directionally selective cells in early cortical areas both project to and receive feedback from cells with large receptive fields that integrate local motion signals to respond to global “object” motion. This type of architecture could satisfy the competing needs to integrate information to resolve ambiguity but, at the same time, maintain the local spatial precision required to represent motion boundaries and features. The perceived direction of motion is therefore an adaptive interplay between both the measurable local signal and its inferred cause.

Keywords: motion—2D, visual cortex, middle vision

Citation: Scarfe, P., & Johnston, A. (2011). Global motion coherence can influence the representation of ambiguous local motion. *Journal of Vision*, 11(12):6, 1–11, <http://www.journalofvision.org/content/11/12/6>, doi:10.1167/11.12.6.

Introduction

One of the primary problems faced by the visual system is the underdetermination of world properties by sensory data (Knill & Richards, 1996; Shams & Beierholm, 2010). A key example of this problem is in motion perception. Ambiguity in motion perception arises for a number of reasons; however, one of the main causes is what has become known as the “aperture problem” (Adelson & Movshon, 1982; Fennema & Thompson, 1979; Marr & Ullman, 1981). The aperture problem refers to the fact that a one-dimensional (1D) image contour viewed through a finite aperture provides no time-varying information parallel to the orientation of the contour. This means that the information available through the aperture is completely ambiguous as to the underlying two-dimensional (2D) motion. In fact, it is equally consistent with an infinite family of 2D motions. Because neurons in early cortical areas, such as V1, have small receptive field sizes compared to image contours, they are subject to the aperture problem and, as a consequence, can predominantly signal only 1D motion orthogonal to image contours spanning their receptive fields (for a comprehensive review, see Pack & Born, 2008).

One way in which this local ambiguity could be overcome is by pooling the response of these cells over orientation and space. This is because with two or more 1D motion signals of different orientations, the underlying

2D motion can be uniquely determined (Adelson & Movshon, 1982). Research has therefore focused on identifying motion-sensitive neurons that could integrate the information available earlier in the motion pathway in order to recover 2D global motion. One area that has been the focus of much research is extrastriate area MT. Cells in MT have large receptive fields that receive feed-forward input from early cortical areas such as V1 (Movshon & Newsome, 1996) and are known to play a significant role in pooling local motion information (Born & Bradley, 2005).

MT has therefore been seen as a candidate site for helping resolve the ambiguity characterizing early motion signals (Movshon, Adelson, Gizzi, & Newsome, 1985; Pack & Born, 2001). In terms of output, MT projects to areas such as MST, which contains cells with large receptive fields that preferentially respond to higher order properties of motion such as patterns of optic flow (Duffy & Wurtz, 1991a, 1991b; Tanaka & Saito, 1989). Overall, this suggests a hierarchical pooling of information through the motion pathway, which works toward resolving the local ambiguity characterizing the response of early cortical areas (Born & Bradley, 2005; Pack & Born, 2008). Note that although one might expect that motion pooling would primarily involve areas V1, MT, and MST, our psychophysical experiments address a more general *processing* architecture in which early ambiguous motion signals are disambiguated through subsequent stages of processing.

While the integration of motion signals is clearly important for the estimation of 2D object motion, the visual system faces the competing need to retain access to spatially precise local information in order to represent motion boundaries and features (Braddick, 1993). This type of information is key to processes such as object segregation and identification (Stoner & Albright, 1996) and is also, in a complementary way, exactly the type of information the visual system needs in order to decide which signals to integrate (Curran, Hibbard, & Johnston, 2007). This points to a tight coupling between integration and segregation in visual motion processing; however, currently there is no clear consensus as to how these competing needs are balanced or the neural architecture that might allow these processes to be instantiated in the brain (Hedges, Stocker, & Simoncelli, 2011; Pack & Born, 2008).

In the present paper, we used global motion Gabor arrays (Amano, Edwards, Badcock, & Nishida, 2009) and the motion aftereffect (Mather, Pavan, Campana, & Casco, 2008; Mather, Verstraten, & Anstis, 1998; Wade, 1994) to help elucidate the interplay between local and global motion processing. Global motion Gabor arrays provide an ideal stimulus because locally each individual Gabor is consistent with an infinite family of possible motions, but when the Gabors in an array are assigned orientations and drift speeds consistent with a single 2D motion solution, the whole array perceptually coheres into a single rigidly moving object/surface (see Amano et al., 2009 for further details). We show that after adaptation to an array such as this, the aftereffect produced by ambiguous local Gabors in the array is shifted toward the global motion direction during adaptation.

This suggests that the visual system is able to use the statistical regularities characterizing 2D global motion to help infer the cause of the ambiguous local signals of which the global motion is composed. This highlights the complex interplay that exists between local and global motion processing and points to a neural architecture in which local directionally coded cells project to, and receive feedback from, cells with large receptive fields that integrate local signals in order to respond to global 2D motion (Sillito, Cudeiro, & Jones, 2006). This type of architecture offers a way in which the visual system might manage the competing requirements to integrate information to reduce ambiguity, but at the same time maintain access to spatially precise local information for tasks such as object segregation.

General methods

Participants

Three participants (AB, AR, and PS) took part in the experiments reported. All were experienced psychophysical

observers. AB was naive to the purposes of the experiment; PS is one of the authors.

Apparatus

Stimuli were presented on a gamma-corrected 20" CRT monitor (Mitsubishi Diamond Plus 230SB) running at 85 Hz with a 1024 × 864 pixel resolution. The stimuli were rendered online in MATLAB (R2009a) using the Psychophysics toolbox extensions (Brainard, 1997; Kleiner, Brainard, & Pelli, 2007; Pelli, 1997). Observers were positioned in a head and chin rest such that a projection from the cyclopean eye intersected normal to the midpoint of the monitor screen. The monitor was viewed at a 40-cm viewing distance. At this distance, the screen spanned approximately 53 × 41 degrees of visual angle. The spatial geometry of the monitor was set so that the pixels were square. Other than the stimulus, the experimental room was completely dark.

Stimuli

The primary stimulus consisted of an annular global motion Gabor array (Amano et al., 2009), in which each Gabor was assigned an orientation and drift speed consistent with an upward 2D drift velocity of 3.2 degrees/s. Each array consisted of 292 Gabors whose orientations were randomly chosen from a uniform distribution spanning ±90 degrees around the global motion direction. Drift speeds were assigned following

$$S_C = S_G \cos(\phi_C - \phi_G), \quad (1)$$

where S_G is the global motion drift speed, ϕ_G is the global motion direction, ϕ_C is the orientation of an individual Gabor element, and S_C is the drift speed it needs to be consistent with the global motion drift velocity. The drift speed of an individual Gabor is therefore a cosine function of the difference between the normal component of the Gabor and the global motion direction, multiplied by the 2D drift velocity. When plotted in velocity space, the vectors for each Gabor fall on a circle through the origin with a diameter equal to the global motion drift speed (Figure 1).

Each Gabor had a spatial frequency of 1.88 cycles per degree, a contrast of 30% and subtended 1.6 degrees of visual angle. There was a 0.1-degree spacing around each Gabor, meaning that the whole array spanned approximately 36 degrees in the horizontal and vertical directions. The diameter of the inner part of the annulus was approximately 19 degrees. The array was centered on the monitor screen on which a black fixation point spanning 0.4 degree was presented throughout. We used an annular structure as Gabors in an array such as this cohere more

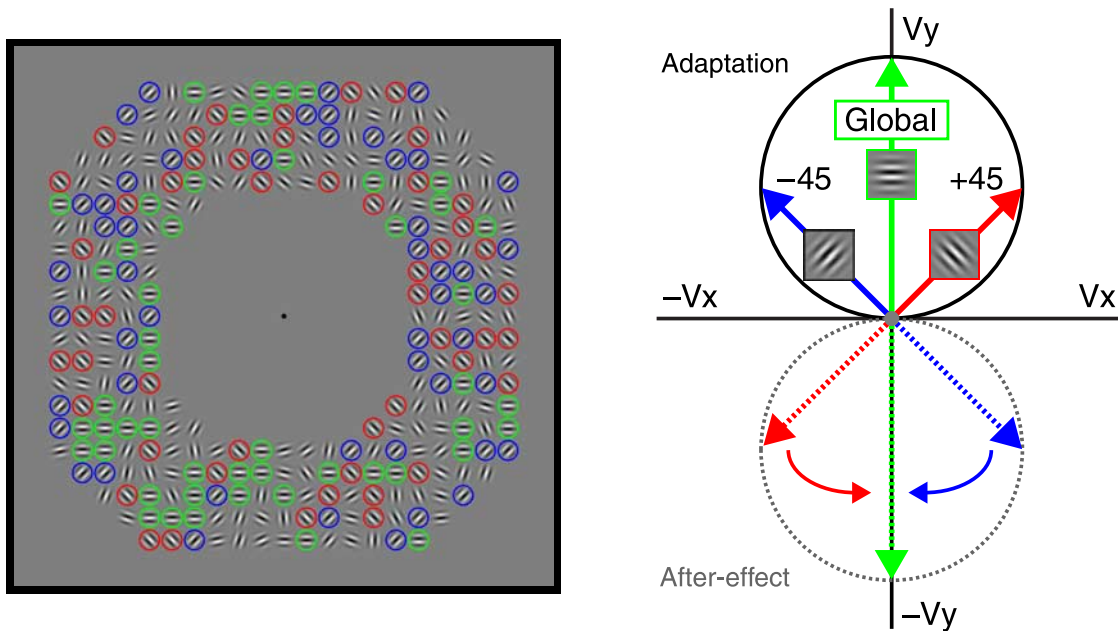


Figure 1. The left panel shows an example of an annular global motion array in which three subsets of Gabors have been highlighted. These subsets are orientated in either the upward global motion direction (Global, green circles) or ± 45 degrees relative to this (Global +45, red circles; Global -45, blue circles). The remaining Gabors making up the array are assigned random orientations drawn from a uniform distribution spanning ± 90 degrees around the global motion direction. The drift speed assigned to each Gabor is a cosine function of the difference between the global motion direction and an angle normal to the Gabors' orientation (Equation 1; Amano et al., 2009). When plotted in velocity space, as shown on the right pane, the vectors describing each Gabor fall on a circle through the origin with a diameter equal to the array's 2D velocity (right panel). The three solid arrows show this schematically for the three subsets of Gabors highlighted in the left-hand panel. The dashed arrows show the predicted local aftereffect direction for each subset, here shown to have the same magnitude. The curved green and blue arrows indicate the direction in which the aftereffects in the ± 45 degree subsets might be modified if they were made more consistent with the global motion direction.

strongly when viewed in the visual periphery, compared to at fixation. The parameters of our array were chosen so that all observers gained a strong percept of coherent upwardly moving global motion for the full duration of each trial during the experiment (see also Amano et al., 2009).

Experiment 1

In [Experiment 1](#), we examined whether the direction of the local MAEs produced by Gabors in a global motion array are influenced by the fact that the local signals in the array are consistent with, and perceived to belong to, a single, rigid, 2D global motion (Amano et al., 2009). We did this by measuring the direction of the motion aftereffect (MAE) produced by three subsets of local Gabor elements placed in our coherently moving arrays. The subsets moved in either the global motion direction or ± 45 degrees relative to this. If the MAE produced by these subsets is caused by a purely local mechanism, its direction should be opposite to the local motion signals present at the test locations during adaptation. If, on the

other hand, the MAE represents an interaction between local and global motion processes, we might predict that the direction of the MAE would be shifted to be more consistent with the global motion direction of which the local signals were part ([Figure 1](#)).

Procedure

Observers adapted to upwardly moving global motion arrays containing our three subsets of test Gabors. Each subset consisted of 50 Gabors randomly distributed within the array ([Figure 1](#)). This meant that there were 142 randomly orientated context Gabors in each array (as detailed above). Adaptation lasted 8 s on the first trial and 3 s on subsequent trials. The Gabors of the array had fixed orientations throughout the whole block, but the phase of each Gabor was randomized on a trial-by-trial basis. After adaptation, we presented a set of static plaids at one of the test subset locations (a different subset in separate blocks of trials). Observers reported the direction of the MAE they observed in the plaids relative to a concurrently seen directional probe ([Figure 2](#)).

The probe consisted of an array of circles 1.6 degrees in diameter, bisected internally by a line defining a specified

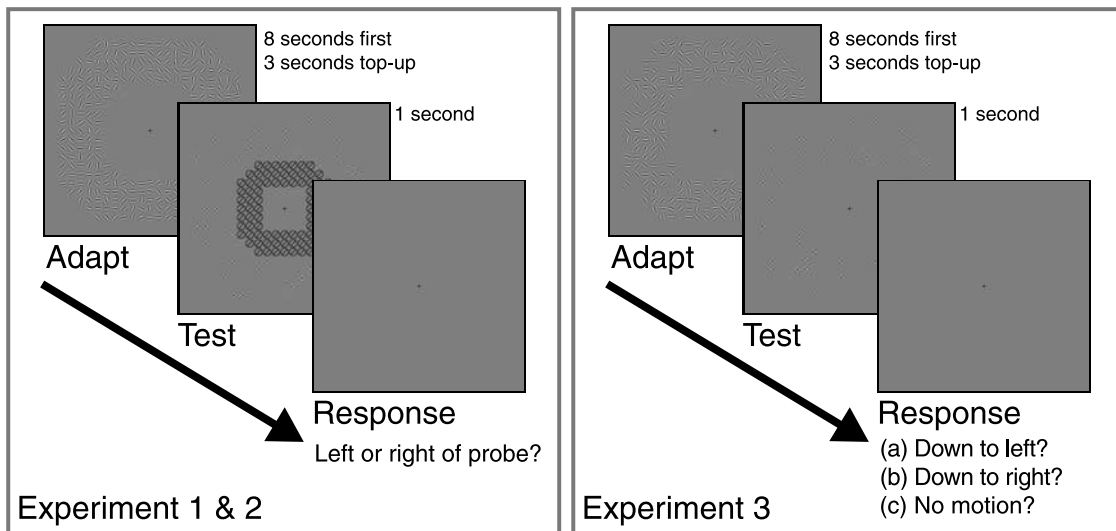


Figure 2. Trial sequence for (left) Experiments 1 and 2 and (right) Experiment 3.

angle. On a given trial, the angle of this line was the same across all elements of the probe array. The observer's task was to judge whether the direction of the MAE observed in the plaids was clockwise or counterclockwise relative to this angle. The component gratings making up the plaids were orientated ± 45 degrees relative to the global motion direction and had the same spatial frequency as the Gabors but an overall contrast of 80%. As with the Gabors, the phase of each of the component gratings making up the plaids were randomized on each trial. The plaids and probe array were presented for 1-s after which time the screen went blank, except for the fixation point. This was a cue for observers to make their response with a keyboard button press.

There was no time limit on observers making their response, but they typically responded immediately (less than a second). This triggered a 1-s intertrial interval before the next adaptation period was presented. Each of the three subsets was tested in a separate block of trials. Within each block, we varied the angle of the directional probe array on each trial using the method of constant stimuli. There were 5 values and each was presented 15 times in a randomized order. The exact values depending on the condition and observer were determined on the basis of pilot experiments. If more than one block was completed in a row, observers took a 2- to 3-min break between blocks with the lights on to minimize dark adaptation.

Results

Cumulative Gaussian functions were fitted to observer's response data in Matlab using the `psignifit` software package (Wichmann & Hill, 2001a, 2001b). From this function, we determined the point of subjective equality (PSE) and bootstrapped 95% confidence intervals around this value. The PSE represents the angle of the directional

probe array that would result in observers responding that the direction of the MAE in the plaids was clockwise or counterclockwise, relative to the directional probe, with equal probability (i.e., the perceived direction of the MAE in the plaids). In Figure 3, we plot psychometric functions and PSEs for each of the three test subsets, for each observer. Within these plots, the functions and PSEs have been normalized to the direction of MAE that would be expected from a purely local mechanism. This means that a normalized aftereffect angle of zero is what one would expect if the direction of the MAE were purely consistent with the local motion signals at the test locations during adaptation.

As can be seen, the functions for the three test subsets are clearly separated along the abscissa. For each observer, the function for the subset moving in the global direction is approximately centered on an aftereffect angle of zero, as would be expected. In contrast, the functions for ± 45 degree subsets are shifted away from each other, in directions consistent with a shift toward the global motion aftereffect direction. These features are clearly shown in the average across observers (Figure 6). This plot shows the mean aftereffect angle for all of our experimental conditions, including those in Experiment 2, as detailed below. The results of Experiment 1 are labeled as "Global." From this graph, it is clear the MAE observers obtained in the ± 45 degree subsets is reliably shifted by around 4 degrees in the direction of the global motion of the adapting array.

The modified MAE that we observe in the global arrays suggests that the visual system is able to use the computational results of global motion processing to help infer the direction of the ambiguous local signals of which the array is composed. However, some alternative hypotheses also present themselves. First, observers might simply be biased in estimating the direction of motion in the ± 45 degree directions such that they underestimate the magnitude of these angles. This would mean that the

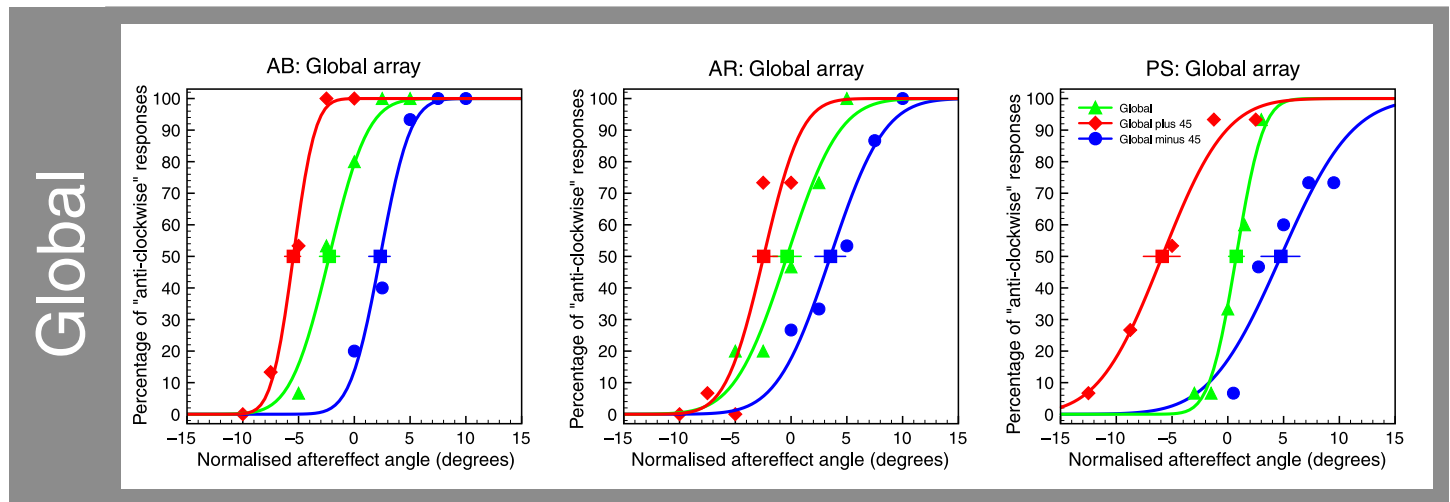


Figure 3. Normalized psychometric functions for the Global array condition. Functions are plotted for each of the three test subsets, with separate graphs for each observer. Squares and horizontal lines show the point of subjective equality (PSE) with bootstrapped 95% confidence intervals.

modified MAE would have had nothing to do with the global motion context during adaptation; instead, it would be due to a simple response bias.

Second, while the modified MAE we observe (and the perceptual coherence of the arrays themselves) suggests that the visual system has access to the conjoint orientation and drift speed of each of the array Gabors, it is also possible that modified MAE could be caused by mechanisms that independently code speed and orientation (Brouwer, Middelburg, Smeets, & Brenner, 2003; Matthews & Qian, 1999; Saffell & Matthews, 2003). For example, a neural mechanism that independently averaged over orientation and used this to modify the orientation of local Gabor elements would also predict the modified direction of MAE that we find.

Finally, the modified MAE could reflect the action of cortical cells with large receptive fields that integrate over sizeable areas of the visual field in order to encode global motions such as optic flow (Duffy & Wurtz, 1991a, 1991b; Tanaka & Saito, 1989). Behavioral evidence for cells such as these comes from the presence of “phantom” motion aftereffects observed in non-adapted regions of large-scale random dot adaptors (Snowden & Milne, 1997). This explanation would also not require the feedback architecture we are considering. Experiments 2 and 3 were designed to test these alternative hypotheses.

Experiment 2

Procedure and results

The procedure for Experiment 2 was identical to that of Experiment 1, except that we now used four different

array types during adaptation. In the first, we simply measured the standard MAE produced from adaptation in each of the three test subsets in isolation, with drift speeds assigned as if they belonged to a global motion array. As expected, the MAE was in the opposite direction to the local motion during adaptation. This is evident in both the individual data (Figure 4) and the group mean (Figure 6), where it is labeled “Standard MAE.” This shows us that when local signals are not part of a global motion array, the MAE is determined purely by the local motion direction at the test locations during adaptation. This rules out the possibility that the modified MAE we found in Experiment 1 was due to a simple response bias. With the following two arrays, we tested the independent coding hypothesis.

The “uniform” arrays were full arrays with identically assigned drift speeds to the standard global motion arrays, but the orientation of all of the Gabors, except the subset being tested, was set so that they faced in the global motion direction. These arrays therefore had the same mean orientation and drift speed as the global motion arrays but failed to cohere into a globally moving surface as the conjoint orientations and drift speeds were no longer consistent with a single 2D motion solution (Adelson & Movshon, 1982; Amano et al., 2009). If the effects we observed in the global arrays were simply due to cells with large receptive fields independently averaging over orientation, the modified MAE should again be observed in the uniform arrays.

This type of averaging would be analogous to some form of “crowding” (Parkes, Lund, Angelucci, Solomon, & Morgan, 2001; Whitney & Levi, 2011). Crowding occurs when the visual system’s ability to resolve properties of individual items, such as their orientation, is lost due to some form of group or ensemble coding (Whitney & Levi, 2011). Importantly, crowding has been shown to

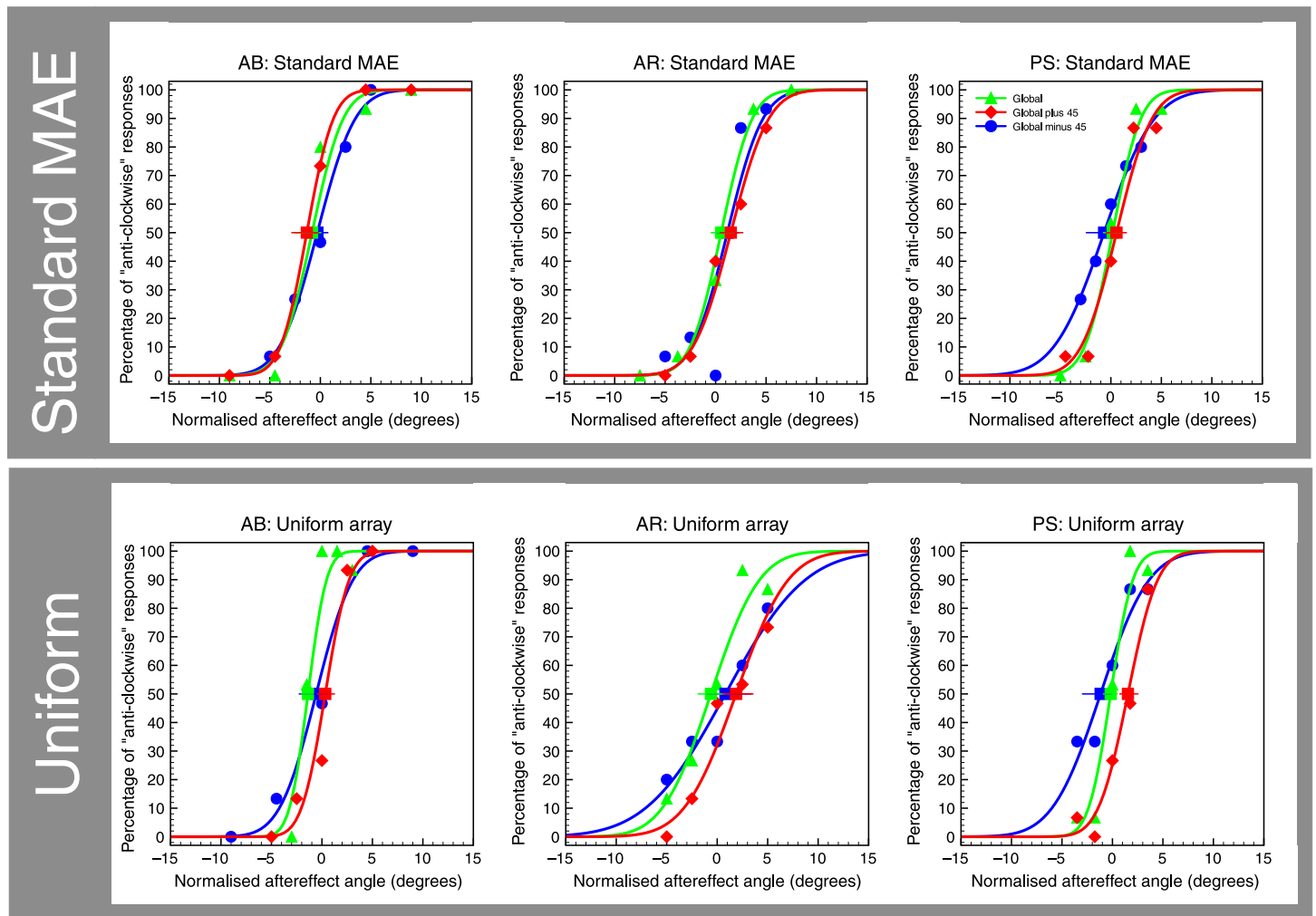


Figure 4. Normalized psychometric functions for the Standard MAE and Uniform array conditions. For each condition, functions are plotted for each of the three test subsets, with separate graphs for each observer. Squares and horizontal lines show the point of subjective equality (PSE) with bootstrapped 95% confidence intervals.

change the orientation of crowded items so that they appear more like the crowding context (Greenwood, Bex, & Dakin, 2010). Contrary to this explanation, the MAE we found in the uniform arrays was purely consistent with the local signals present at the test locations during adaptation. This is evident in both the individual (Figure 4) and group data (Figure 6). Failure to find a modified local MAE in the uniform arrays suggests that an independent mechanism averaging over orientation is unable to account for our data. However, there was an important difference between the uniform arrays and the global motion arrays.

While the uniform arrays had the same distribution of drift speeds to the global motion arrays, the distribution of component motions in the global motion direction was not the same. If the modified MAE we observed in the global arrays was caused by local interactions between component motions in the global motion direction, rather than the perceptual coherence of the array *per se*, this could

account for our data. In order to control for this possibility, we measured the direction of the local MAE in what we term “component” arrays. These were similar to the uniform arrays, in that we again set all of the Gabors, except the subset being tested, so that they faced the global motion direction. However, we now assigned drift speeds to these uniformly orientated Gabors such that they had the same component motion in the global motion direction as in a standard global motion array.

This was done by assigning drift speeds as a function of the squared cosine difference between the normal component of the Gabor and the global motion direction, multiplied by the 2D drift velocity (Scarfe & Johnston, 2010):

$$S_C = S_G \cos^2(\phi_C - \phi_G). \quad (2)$$

Equation 2 follows the same format as Equation 1. S_G is the global motion drift speed and ϕ_G is the global motion

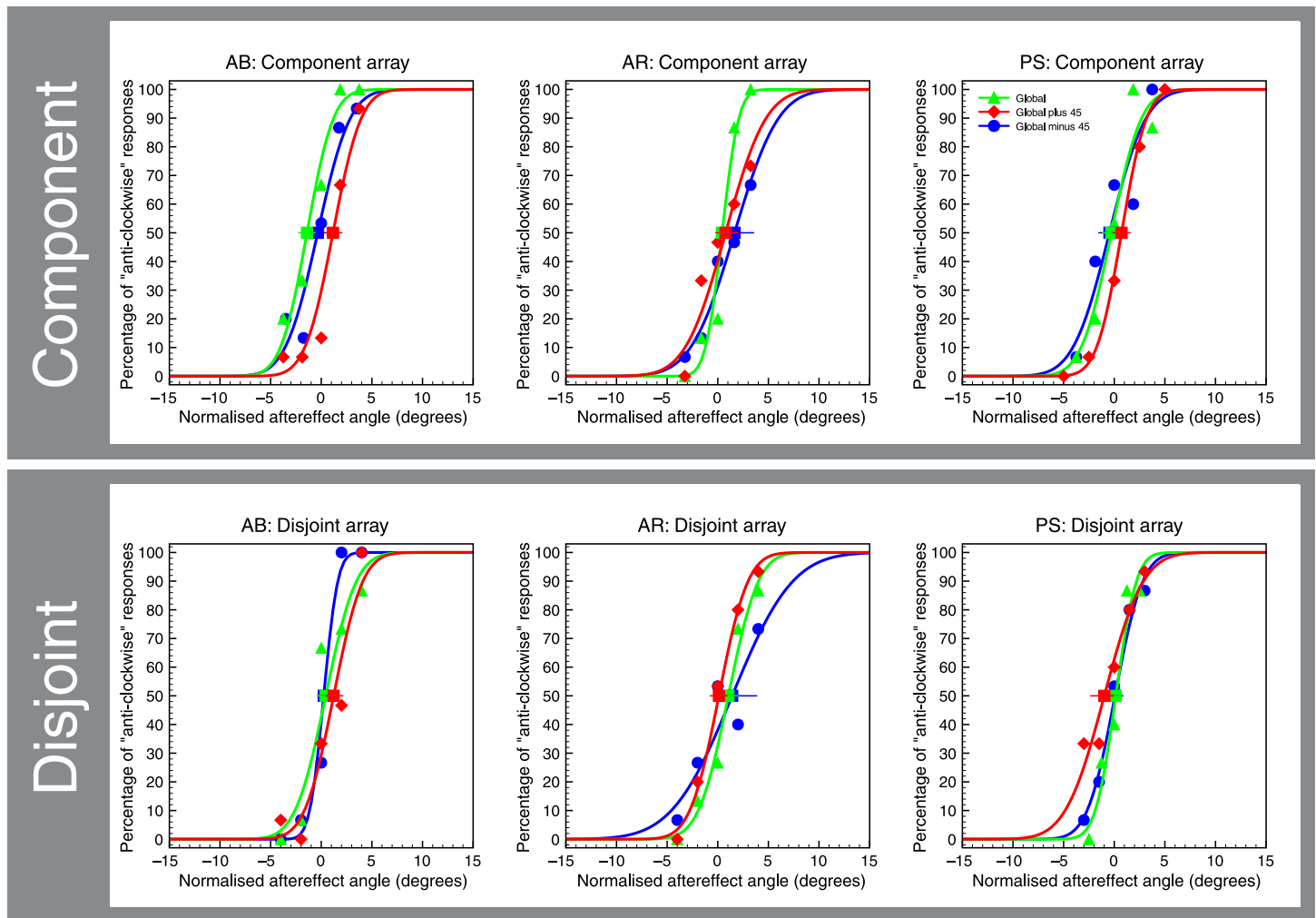


Figure 5. Normalized psychometric functions for the Component and Disjoint array conditions. For each condition, functions are plotted for each of the three test subsets, with separate graphs for each observer. Squares and horizontal lines show the point of subjective equality (PSE) with bootstrapped 95% confidence intervals.

direction, whereas ϕ_C is the orientation of an individual Gabor element and S_C is that element's drift speed. Assigning drift speeds in this way allowed us to match the distribution of local component motions in the global motion direction to that found in a standard global motion array. Any effects based on these component motions would therefore be identical across both types of array. Contrary to this hypothesis, Figures 5 and 6 show that the MAE we observe in the component arrays is again purely consistent with the local motions at the test locations during adaptation.

As a final control, we constructed arrays in which the orientation and drift speed statistics were *both* identical to the global motion arrays but were again inconsistent with a 2D global motion solution. We did this by assigning orientations and drift speeds with different random selections from the uniform ± 90 degree distribution around the global motion direction. As such, we label

these as “disjoint” arrays. To any mechanism responding independently to orientation or drift speed (Brouwer et al., 2003; Matthews & Qian, 1999; Saffell & Matthews, 2003), these arrays would be indistinguishable to the standard global motion arrays; however, because the orientations and drift speed were no longer consistent with a single 2D motion, they again failed to cohere into a single rigidly moving surface. Figures 5 and 6 show that the MAE we observe in the disjoint arrays was again purely consistent with the local motions at the test locations during adaptation.

With Experiment 2, we were therefore able to rule out two alternative hypotheses for the modified MAE we observed in Experiment 1. The first was that the modified MAE was simply due to a response bias. The second was that mechanisms independently averaging over orientation or drift speed could account for the modified MAE (Brouwer et al., 2003; Matthews & Qian, 1999; Saffell & Matthews, 2003). In Experiment 3, we examined

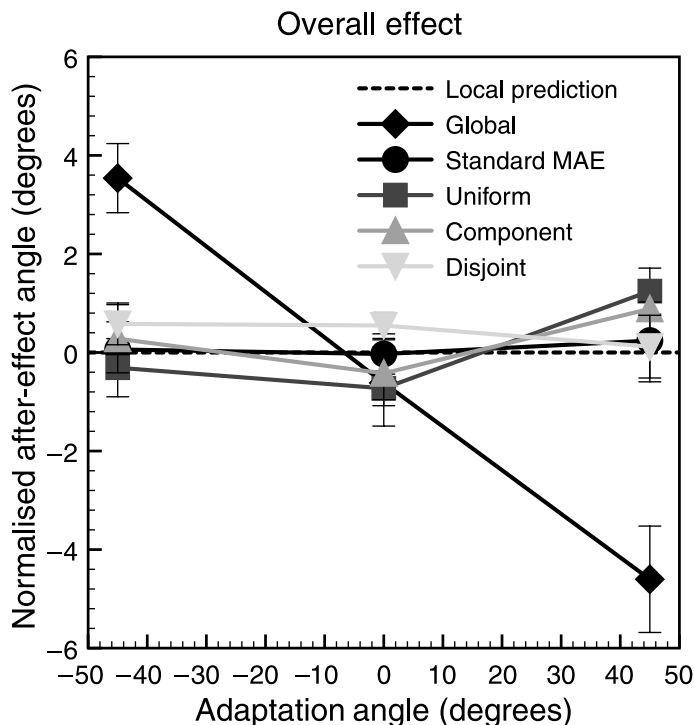


Figure 6. Mean normalized aftereffect angle across observers for Experiments 1 and 2. Error bars show standard error of the mean. See accompanying text for details.

whether cells with large receptive fields selectively responsive to optic flow could account for our data (Snowden & Milne, 1997).

Experiment 3

In Experiment 3, we looked for the presence of phantom motion aftereffects in gaps placed within our arrays. If we found phantom MAEs, this would suggest that our results could be accounted for by the action of extrastriate cells with large receptive fields that selectively respond to optic flow. We were not sure this would be the case for a number of reasons. First, research has shown that global pooling can operate differently in the case of locally 2D (dots and plaids) and locally 1D (Gabor) pattern elements (Amano et al., 2009). This means that results gained using locally 2D stimuli might not be readily generalizable to our locally ambiguous 1D Gabors. Second, some authors have failed to find phantom MAEs with translating stimuli, as compared to stimuli that contain global expansion (Meng, Mazzoni, & Qian, 2006).

Procedure

Observers adapted to an upwardly moving global motion array, in which we placed two subsets of 50 Gabors

moving ± 45 degrees relative to the global motion direction, and an equal number of array gaps, where no Gabors were present (Figure 7). As in Experiment 1, we subsequently presented test plaids at each of these locations to test for the presence and direction of a motion aftereffect. The experimental timings and all characteristics of the Gabors and plaids were identical to Experiments 1 and 2. We did however adopt a different experimental procedure and response methodology.

We presented test plaids independently at each of the three test subset locations randomly interleaved in a single block of trials. Each subset was tested 25 times, making 75 trials in total. The observer's task was to respond whether the MAE they observed in the plaids produced motion "down to the left," "down to the right," or no motion at all. They made their response with a keyboard button press, which triggered a 1-s intertrial interval before the next trial began. We adopted this 3AFC procedure rather than using the direction probe array we had used in Experiments 1 and 2, because pilot studies had shown that observers robustly perceived no motion when gap locations were tested. It therefore felt very odd to our observers to be "guessing" the direction of motion relative to the directional probe when in fact they saw absolutely no motion.

The results of Experiments 1 and 2 had shown that observers robustly perceived a MAE "down to the left" with the +45 degree subset and "down to the right" with the -45 degree subset (Figures 3–6), so we could be confident that when motion was perceived, it would fit into these two broad categories. We were also able to confirm this when our observers were debriefed at the end of the experiment. None of our observers had any difficulty in using the three response categories. We made the decision to *replace* the subset moving in the global motion direction with array gaps rather than add a subset of gaps *in addition* to the subset moving in the global motion direction, so as to maintain the same number of context Gabors to that used in Experiments 1 and 2.

Results

The results were very clear and are shown in Figure 7. When the ± 45 degree subset locations were tested, observers perceived motion in the predicted directions on virtually 100% of trials. In contrast, when the gap locations were tested, observers universally perceived no motion. This suggests that the modified MAE that we found in Experiment 1 cannot be accounted for by the adaptation of extrastriate cells selectively responsive to optic flow (Snowden & Milne, 1997). It is also consistent with previous results that have failed to find phantom MAEs with globally translating stimuli (Meng et al., 2006).

Failure to find phantom MAEs at gaps in our arrays may be due to the local ambiguity of Gabors encouraging

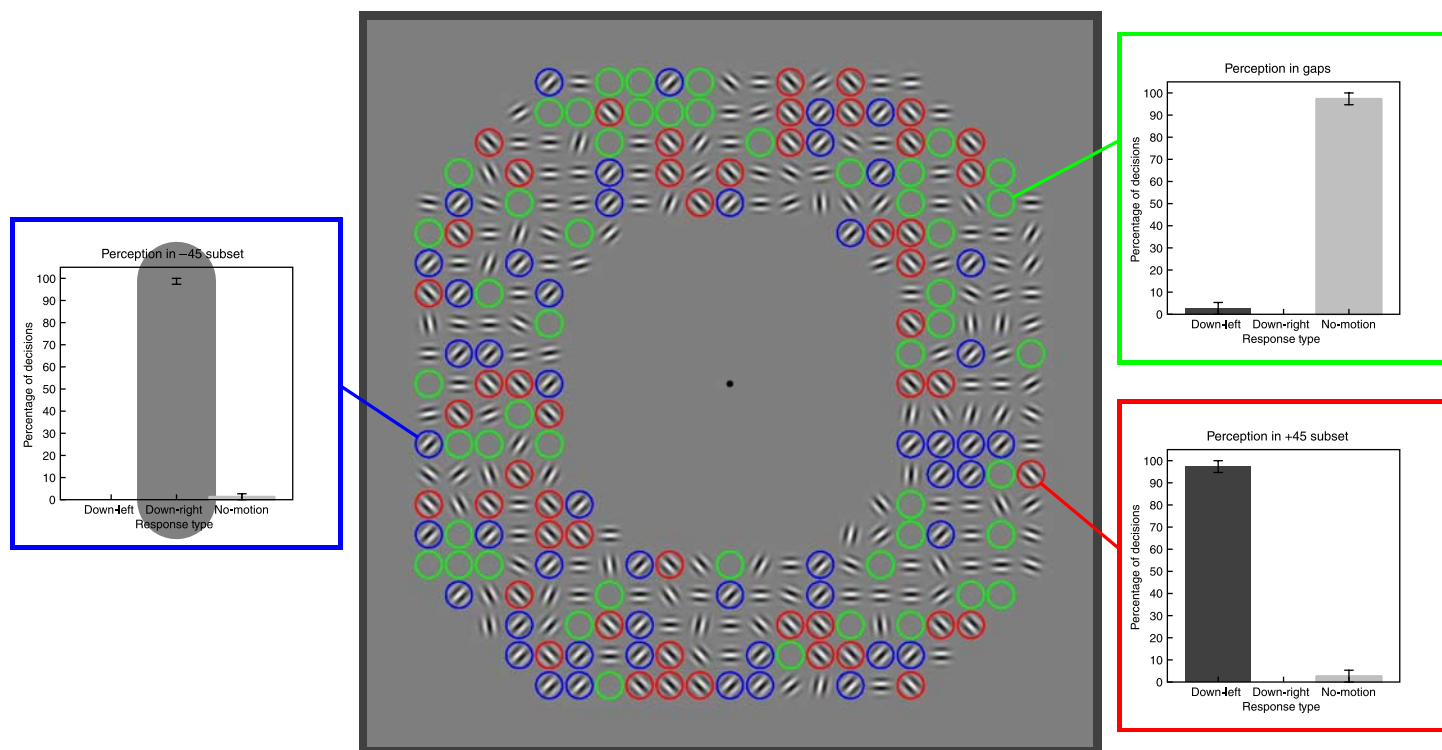


Figure 7. Diagram showing a Global motion Gabor array containing a set of array gaps, as used in Experiment 3. The inset graphs show the proportion of “down-left,” “down-right,” and “no motion” decisions for the three test subsets (± 45 degrees and gaps).

segregation, due to consistency with 2D object motion rather than indiscriminate integration, which seems to characterize locally 2D signals (Snowden & Milne, 1997). Previous results have shown that motion integration can operate different on locally 1D and locally 2D stimuli (Amano et al., 2009). Cells with large receptive fields selectively responsive to motion can also show spatially specific adaptation effects within their receptive fields (Kohn & Movshon, 2003; Pack, Born, & Livingstone, 2003). This means that although these cells respond to motion at multiple spatial locations, they do not integrate in a uniform way across their whole receptive field. Spatially specific adaptation presumably reflects adaptation in cells with small receptive fields that project to the higher order cell.

Discussion

The ambiguity of local 1D motion signals is one of the primary problems the visual system must overcome if it is to accurately estimate the underlying 2D motion in the environment. Here, we show that the aftereffect produced by ambiguous local motion signals is modified to be more consistent with the global motion of which those local signals were part. This suggests that the visual system

uses the outcome of global motion processing to help infer the cause of measured ambiguous local motion information. The modified MAE we observed could not be explained by local adaptation or a simple response bias and was inconsistent with being mediated by mechanisms independently coding orientation and speed (Brouwer et al., 2003; Matthews & Qian, 1999; Saffell & Matthews, 2003). It was also inconsistent with the adaptation of extrastriate cells that integrate local 2D motion signals over large regions of space in order to respond to global flow properties (Snowden & Milne, 1997).

Instead, our data suggest a neural architecture whereby directionally coded cells both project to and receive feedback from cells with large receptive fields that are sensitive to the statistical regularities characterizing 2D global motion. This could occur through the numerous feedback connections that exist between extrastriate areas such as MT/MST, which respond to global motion, and early cortical areas such as V1 that represent motion locally (Nishida & Johnston, 1999; Sillito et al., 2006). This interaction between the coding of local and global motion would also allow the visual system to balance the competing requirements to integrate information over space to encode global motion, while at the same time retain the local precision required to represent boundaries and features (Braddick, 1993). Along with previous research, this shows that the MAE is more than a simple competitive interaction between populations of cells

coding different local motion directions (Culham et al., 1999). Instead, it shows that a perceived direction of motion is an adaptive interplay between both the measurable local signal and its globally inferred cause.

Acknowledgments

The authors would like to thank Dr. Harry Griffin and other members of the Vision Lab at UCL for helpful discussions regarding the research presented in this manuscript. The research was supported by a grant from the BBSRC.

Commercial relationships: none.

Corresponding author: Peter Scarfe.

Email: p.scarfe@ucl.ac.uk.

Address: Department of Cognitive, Perceptual and Brain Sciences, University College London, 26 Bedford Way, London, WC1H 0AP, UK.

References

- Adelson, E. H., & Movshon, J. A. (1982). Phenomenal coherence of moving visual patterns. *Nature*, *300*, 523–525.
- Amano, K., Edwards, M., Badcock, D. R., & Nishida, S. (2009). Adaptive pooling of visual motion signals by the human visual system revealed with a novel multi-element stimulus. *Journal of Vision*, *9*(3):4, 1–25, <http://www.journalofvision.org/content/9/3/4>, doi:10.1167/9.3.4. [PubMed] [Article]
- Born, R. T., & Bradley, D. C. (2005). Structure and function of visual area MT. *Annual Review of Neuroscience*, *28*, 157–189.
- Braddick, O. (1993). Segmentation versus integration in visual motion processing. *Trends in Neurosciences*, *16*, 263–268.
- Brainard, D. H. (1997). The psychophysics toolbox. *Spatial Vision*, *10*, 433–436.
- Brouwer, A. M., Middelburg, T., Smeets, J. B., & Brenner, E. (2003). Hitting moving targets: A dissociation between the use of the target's speed and direction of motion. *Experimental Brain Research. Experimentelle Hirnforschung. Experimentation Cerebrale*, *152*, 368–375.
- Culham, J. C., Dukelow, S. P., Vilis, T., Hassard, F. A., Gati, J. S., Menon, R. S., et al. (1999). Recovery of fMRI activation in motion area MT following storage of the motion aftereffect. *Journal of Neurophysiology*, *81*, 388–393.
- Curran, W., Hibbard, P. B., & Johnston, A. (2007). The visual processing of motion-defined transparency. *Proceedings of the Royal Society of London B: Biological Sciences*, *274*, 1049–1056.
- Duffy, C. J., & Wurtz, R. H. (1991a). Sensitivity of MST neurons to optic flow stimuli: I. A continuum of response selectivity to large-field stimuli. *Journal of Neurophysiology*, *65*, 1329–1345.
- Duffy, C. J., & Wurtz, R. H. (1991b). Sensitivity of MST neurons to optic flow stimuli: II. Mechanisms of response selectivity revealed by small-field stimuli. *Journal of Neurophysiology*, *65*, 1346–1359.
- Fennema, C. L., & Thompson, W. B. (1979). Velocity determination in scenes containing several moving objects. *Computer Graphics and Image Processing*, *9*, 301–315.
- Greenwood, J. A., Bex, P. J., & Dakin, S. C. (2010). Crowding changes appearance. *Current Biology*, *20*, 496–501.
- Hedges, J. H., Stocker, A. A., & Simoncelli, E. P. (2011). Optimal inference explains the perceptual coherence of visual motion stimuli. *Journal of Vision*, *11*(6):14, 1–16, <http://www.journalofvision.org/content/11/6/14>, doi:10.1167/11.6.14. [PubMed] [Article]
- Kleiner, M., Brainard, D., & Pelli, D. (2007). What's new in Psychtoolbox-3? [Meeting Abstract]. *Perception*, *36*, 14–14.
- Knill, D. C., & Richards, W. (1996). *Perception as Bayesian inference*. Cambridge, UK: Cambridge University Press.
- Kohn, A., & Movshon, J. A. (2003). Neuronal adaptation to visual motion in area MT of the macaque. *Neuron*, *39*, 681–691.
- Marr, D., & Ullman, S. (1981). Directional selectivity and its use in early visual processing. *Proceedings of the Royal Society of London B: Containing Papers of a Biological Character*, *211*, 151–180.
- Mather, G., Pavan, A., Campana, G., & Casco, C. (2008). The motion aftereffect reloaded. *Trends in Cognitive Sciences*, *12*, 481–487.
- Mather, G., Verstraten, F., & Anstis, S. (1998). *The motion aftereffect: A modern perspective*. Cambridge, MA: MIT Press.
- Matthews, N., & Qian, N. (1999). Axis-of-motion affects direction discrimination, not speed discrimination. *Vision Research*, *39*, 2205–2211.
- Meng, X., Mazoni, P., & Qian, N. (2006). Cross-fixation transfer of motion aftereffects with expansion motion. *Vision Research*, *46*, 3681–3689.
- Movshon, J. A., Adelson, E. H., Gizzi, M. S., & Newsome, W. T. (1985). The analysis of moving visual patterns. *Pattern Recognition Mechanisms*, *54*, 117–151.
- Movshon, J. A., & Newsome, W. T. (1996). Visual response properties of striate cortical neurons projecting to

- area MT in macaque monkeys. *Journal of Neuroscience*, *16*, 7733–7741.
- Nishida, S., & Johnston, A. (1999). Influence of motion signals on the perceived position of spatial pattern. *Nature*, *397*, 610–612.
- Pack, C. C., & Born, R. T. (2001). Temporal dynamics of a neural solution to the aperture problem in visual area MT of macaque brain. *Nature*, *409*, 1040–1042.
- Pack, C. C., & Born, R. T. (2008). Cortical mechanisms for the integration of visual motion. In R. H. Masl & T. Albright (Eds.), *The senses: A comprehensive reference* (vol. 2, pp. 189–218). San Diego, CA: Academic Press.
- Pack, C. C., Born, R. T., & Livingstone, M. S. (2003). Two-dimensional substructure of stereo and motion interactions in macaque visual cortex. *Neuron*, *37*, 525–535.
- Parkes, L., Lund, J., Angelucci, A., Solomon, J. A., & Morgan, M. (2001). Compulsory averaging of crowded orientation signals in human vision. *Nature Neuroscience*, *4*, 739–744.
- Pelli, D. G. (1997). The VideoToolbox software for visual psychophysics: Transforming numbers into movies. *Spatial Vision*, *10*, 437–442.
- Saffell, T., & Matthews, N. (2003). Task-specific perceptual learning on speed and direction discrimination. *Vision Research*, *43*, 1365–1374.
- Scarfe, P., & Johnston, A. (2010). Motion drag induced by global motion Gabor arrays. *Journal of Vision*, *10*(5):4, 1–15, <http://www.journalofvision.org/content/10/5/14>, doi:10.1167/10.5.14. [PubMed] [Article]
- Shams, L., & Beierholm, U. R. (2010). Causal inference in perception. *Trends in Cognitive Sciences*, *14*, 425–432.
- Sillito, A. M., Cudeiro, J., & Jones, H. E. (2006). Always returning: Feedback and sensory processing in visual cortex and thalamus. [Review]. *Trends in Neurosciences*, *29*, 307–316.
- Snowden, R. J., & Milne, A. B. (1997). Phantom motion aftereffects—Evidence of detectors for the analysis of optic flow. *Current Biology*, *7*, 717–722.
- Stoner, G. R., & Albright, T. D. (1996). The interpretation of visual motion: Evidence for surface segmentation mechanisms. *Vision Research*, *36*, 1291–1310.
- Tanaka, K., & Saito, H. (1989). Analysis of motion of the visual field by direction, expansion/contraction, and rotation cells clustered in the dorsal part of the medial superior temporal area of the macaque monkey. *Journal of Neurophysiology*, *62*, 626–641.
- Wade, N. J. (1994). A selective history of the study of visual motion aftereffects. *Perception*, *23*, 1111–1134.
- Whitney, D., & Levi, D. M. (2011). Visual crowding: A fundamental limit on conscious perception and object recognition. *Trends in Cognitive Sciences*, *15*, 160–168.
- Wichmann, F. A., & Hill, N. J. (2001a). The psychometric function: I. Fitting, sampling, and goodness of fit. *Perception & Psychophysics*, *63*, 1293–1313.
- Wichmann, F. A., & Hill, N. J. (2001b). The psychometric function: II. Bootstrap-based confidence intervals and sampling. *Perception & Psychophysics*, *63*, 1314–1329.